

Closure Report 2017-2020

Title: Multicomponent Crystal Technology to Improve Drug Pharmacokinetic Attributes.
CSIR Project File No. 02(0327)/17/EMR-II

Dated: 08/11/2017

PI: Dr. Bipul Chandra Sarma

Address: Department of Chemical Sciences, Tezpur University

Napam, Tezpur-784028, Assam, India

Email: bcsarma@tezu.ernet.in

Summary of work done: The use of supramolecular chemistry and crystal engineering to improve drug pharmacokinetics aspect is an area of great scientific and technological interest. The presence of hydrogen bond synthon and π -stacking are considered as two important adhesive and cohesive tools in the crystallization of drug molecules. In order to establish the proposed objectives of the present project work, we have explored synthesis of drug cocrystals/salts with emphasized pharmacokinetic properties. The overall summary of work done during the tenure of the project is given below:

1. Review article entitled "Drug-Drug and Drug-Nutraceutical Cocrystal/Salt as Alternative Medicine for Combination Therapy: A Crystal Engineering Approach". Herein, we discussed case studies of drug-drug, drug-nutraceutical cocrystals, and a few salts with an emphasis on their role in physicochemical property modulation. The strategy involved in drug-coformer combinations have shown significant potential of forming energetically and structurally robust interactions that are highlighted as the use of hydrogen bonding and crystal engineering strategies to improve the drug profile. **(Published paper)**
2. Regulation of $\pi \cdots \pi$ stacking interactions in small molecule cocrystals and/or salts for physiochemical property modulation: We employed acridine as a cocrystal partner with an isomer of dihydroxybenzoic acid coformer and used crystal engineering approaches to improve drug properties. Here, the role of $\pi \cdots \pi$ stacking and hydrogen bonding interactions played vital role in the crystallization of small drug molecules to regulate certain physiochemical properties of multicomponent crystals. **(Published paper)**
3. Trimorphic ethenzamide cocrystal: in-vitro solubility and membrane efflux studies: We demonstrated another cocrystal system with drug ethenzamide (ZMD) and 2,4-Dihydroxybenzoic acid coformer for better understanding the bioavailability of cocrystal polymorphs. With the variation of crystallization media and stoichiometric ratio, we established a trimorphic form of ZMD-2,4-DHBA cocrystals. In this system, we improved physiochemical properties of synthesized cocrystal by understanding different physical parameters such as solute-solvent interaction, molecular symmetry, and hydrogen bond synthon as well as particle size distribution. **(Published paper)**
4. Mechanistic Study on Stability Enhancement of Drug Famotidine by Cocrystallization: Structure-Activity, Stability and Pharmacokinetics Correlations: We further synthesized famotidine cocrystals using three different xanthine derivatives such as caffeine; theophylline and theobromine followed by phase stability studies at physiological pH environment. Formation of strong intermolecular interactions in the crystal structure of famotidine:theophylline cocrystal emphasized additional

Bipul Sarma

phase stability by concealing the acid hydrolysis of imines moiety of drug famotidine. (Published paper)

5. Control concomitant polymorphism system: Short-acting antimicrobial sulfa drug sulfathiazole is known for its concomitant crystallization with five existing polymorphs due to conformational flexibility and hydrogen bond synthon variation. The issue of concomitant crystallization of a drug in its development stage needs to be addressed for patent litigation that includes legal actions to protect patents against infringement. Functional self-assembled monolayer (SAM) of organic thiol on gold surface has been employed as an efficient approach to control concomitant nucleation of such flexible drug and emphasized. The crystallization on SAM surface is mostly kinetically driven and often nucleates novel metastable forms. (Published paper)
6. Book Chapter on "Nanocarriers in drug-delivery system: eminence and confront". Nanocarriers proponents have gained major attentions in pharmaceutical drug delivery due to the presence of various advantages such as improve drug stability, ability of drug targeting and bioavailability etc. The rational design of nanocarriers improves the major targets of ingredients such as specific targeted sites, therapeutic and diagnostic modalities, efficacy and safety. It can be stimulated by understanding the relationship between pharmacokinetic and pharmacodynamic profile of drugs. Therefore, this chapter emphasizes a succinct endeavor of ill-famed nanomedicine through the improvement of their delivery challenges with high efficacy and wide safety margin which was developed in the past decades. It helps to understand the overall beneficial therapeutic index of new or active ingredients. (Published)
7. Article on "Variable stoichiometry cocrystals: occurrence and significance". A review on different stoichiometry cocrystals reported mostly in the last decade to elucidate the factors responsible for their formation, with an intention to address an imperative issue in the drug development process. The effects of solvents and cofomer concentration on cocrystal stability have been highlighted along with the impacts of variable stoichiometry on physicochemical properties. (Published Paper)
8. Book Chapter on 'Crystal engineering and pharmaceutical crystallization': This chapter has covered the principles of cocrystal and salt design to their applications in pharmaceuticals and manufacturing improvements with continuous-flow processes. (Published Paper)
9. Book Chapter on "Multicomponent Crystalline Solids: A Pre-Formulation to Discover Alternate Combination Drug". This review confers the present scenario on recent progresses of multicomponent crystalline solids especially cocrystals in pharmaceutical developments with an emphasis of cooperative efforts to discover an alternate hybrid drug. Recent examples, new synthetic strategies, advanced structural characterization techniques and future of multicomponent crystals for healthcare department are important wedges in this review. It is anticipated that this article will guide various approaches intended for better understanding of new drug phase. (Minor revision submitted)

Additional work with acknowledgment: Drug development is an extensive process and the pre-formulations often developed are found to inherit components that interfere with nucleation in the crystallization batches. Considering the robustness and utility of covalent organic frameworks (COF) – a new age material, we have attempted to synthesize various such porous materials for the purpose of selective purification and separation. While the progress in this field is taking shape, in the meantime we have reported efficient catalytic potentials of the COF materials.

1. Cu(II) Complex onto a Pyridine-Based Porous Organic Polymer as a Heterogeneous Catalyst for Nitroarene Reduction: A Cu(II) catalyst incorporated onto a new pyridine based porous organic

polymer linked by carboxamide functionality has been developed. The synthesized catalyst represents a better atom economy and provides a greener and efficient pathway towards nitroarene reduction, as an alternative to expensive metal catalysts in use. (Published Paper)

2. Endorsing Organic Porous Polymers in Regioselective and Unusual Oxidative C=C Bond Cleavage of Styrenes into Aldehydes and Anaerobic Benzyl Alcohol Oxidation via Hydride Elimination: Regioselective oxidative cleavage of styrene C=C bond in a first of its kind reaction by a nitrogen-rich triazine-based microporous organic polymer without metal add-ons is reported in this paper. The framework material further shows high catalytic efficiency in an anaerobic oxidation reaction of benzyl alcohols into benzaldehydes. Essentially, the study unveils protruding applications of metal-free nitrogen-rich porous polymers in organic transformation reactions. (Published Paper)

List of publications (copy of the 1st & acknowledgement pages enclosed):

1. Ranjit Thakuria and Bipul Sarma, Drug-Drug and Drug-Nutraceutical Cocrystal/Salt as Alternative Medicine for Combination Therapy: A Crystal Engineering Approach; *Crystals*, 2018, 8, 2, 101-.
2. Pranita Bora, Basanta Saikia and Bipul Sarma, Regulation of $\pi \cdots \pi$ stacking interactions in small molecule cocrystals and/or salts for physiochemical property modulation; *Cryst. Growth Des.*, 2018, 18, 3, 1448-1458.
3. Rajiv Khatioda, Pranita Bora and Bipul Sarma, Trimorphic ethenzamide cocrystal: *in-vitro* solubility and membrane efflux studies; *Cryst. Growth Des.*, 2018, 18, 8, 4637-4645.
4. Basanta Saikia, Nazima Sultana, Trisha Kaushik, Bipul Sarma, Mechanistic Study on Stability Enhancement of Drug Famotidine by Cocrystallization: Structure-Activity, Stability and Pharmacokinetics Correlations *Cryst. Growth Des.*, 2019, 19, 11, 6472-6481.
5. Pranita Bora, Basanta Saikia and Bipul Sarma, Oriented crystallization on organic monolayers to control concomitant polymorphism; *Chem. Eur. J.*, 2019.
6. Nazima Sultana, Pranita Bora, Bipul Sarma, Smart Nanocontainers: Fundamental and Emerging Application; Chapter 10: Nanocarriers in Drug Delivery: Eminence and Confront: 1st Edition; Elsevier; *Micro and Nano Technologies*, ISBN: 9780128167700, 2020, 159-178.
7. Basanta Saikia, Debabrat Pathak, Bipul Sarma, Variable stoichiometry cocrystals: Occurrence and Significance; *CrystEngComm*, 2021, 23, 4583-4606.
8. Geetha Bolla, Bipul Sarma, Ashwini K. Nangia, Hot Topics in Crystal Engineering; Chapter 5: Crystal engineering and pharmaceutical crystallization; Elsevier; ISBN: 978-0-12-818192-8, 2021, 157-229.
9. Rajiv Khatioda, Debabrat Pathak, Bipul Sarma, Cu(II) Complex onto a Pyridine-Based Porous Organic Polymer as a Heterogeneous Catalyst for Nitroarene Reduction; *ChemistrySelect*, 2018, 3, 23, 6309-6320.
10. Debabrat Pathak, Rajiv Khatioda, Himanshu Sharma, Ankur K. Guha, Lakshi Saikia, Bipul Sarma, Endorsing Organic Porous Polymers in Regioselective and Unusual Oxidative C=C Bond Cleavage of Styrenes into Aldehydes and Anaerobic Benzyl Alcohol Oxidation via Hydride Elimination; *ACS Appl. Mater. Interfaces*, 2021, 13, 13, 15353-15365.

Detailed Progress Report:

1. **Drug Drug and Drug Nutraceutical Cocrystal/Salt as Alternative Medicine for Combination Therapy: A Crystal Engineering Approach:** The pre-formulation of pharmaceutical solids is a concept of crystal engineering that has emerged as a promising technique for drug development in the pharmaceutical industry. Recent introduction of pharmaceutical cocrystals in regulatory guidelines of US Food and Drug Administration (FDA) made them one of the potent alternatives when salt preparation is not feasible. Apart from generally regarded as safe (GRAS) cofomers, drug-drug and drug-nutraceutical cocrystals are recent additions to pharmaceutical cocrystal family that have additional health benefits.

Bipul Sarma

Indeed, preparation of salt forms is a routine practice to deal with inadequacies associated with the active pharmaceutical ingredient (API) and happens to be a potentially reliable method. Amongst them, drug-pharmaceutical ingredient (API) and happens to be a potentially reliable method. Amongst them, drug-drug and drug-nutraceutical cocrystals have drawn significant importance in the recent past as they reduce drug load and cost effects during multiple disease diagnosis. However, one has to be prudent in the selection of drug molecules, the presence of complementary hydrogen bond synthon, disease management during multiple disease therapy, etc. that play important roles in their preparation. That is the reason why drug-drug cocrystals are scarce in the literature compared to pharmaceutical cocrystals containing GRAS cofomers and salt forms. Therefore, this review paper mainly highlighted the different case studies that preferably reported drug-drug, drug-nutraceutical cocrystals, and a few salts with an emphasis on their role in physicochemical property modulation. It will help researcher to design viable alternative to traditional drugs in the near future.

2. Regulation of $\pi \cdots \pi$ stacking interactions in small molecule cocrystals and/or salts for physicochemical property modulation: We demonstrated the role of $\pi \cdots \pi$ stacking interaction to regulate desired physicochemical properties of the multicomponent crystals. The product materials of Acridine (Acr) with six different isomeric dihydroxy benzoic acids (DHBA) namely CC-1 [Acr·2,3-DHBA], CC-2 [Acr·2,4-DHBA], CC-3 [Acr·2,5-DHBA], CC-4 [Acr·2,6-DHBA], CC-5 [Acr·3,4-DHBA] and CC-6 [Acr·3,5-DHBA] were prepared by using mechanochemical neat grinding method. They were characterized using different spectroscopic techniques like thermal analysis, FT-IR spectroscopy, PXRD and SCXRD etc. In FT-IR absorption band, the appearance of major vibrational frequency at 3041 and 1512 cm^{-1} indicates the presence of aromatic C-H and C-N group respectively for acridine molecule. The vibrational frequencies of those particular peaks were shifted to 3043, 3044, 3044, 3050, 3057, 3051 cm^{-1} and 1319, 1308, 1343, 1346, 1377, 1331 cm^{-1} respectively for CC-1 to CC-6 (Figure 1A). The DSC thermograms of the prepared cocrystals were shown in Figure 1B. In Figure 1B, the measured onset and sharp peak maximum of the melting endotherms were introduced from the formation of new cocrystals. The PXRD diffraction spectra of CC-1 to CC-6 had numerous distinct peaks indicating the high crystalline state of the materials (Figure 2A). SCXRD data were collected for the prepared cocrystals. The crystal structure reveals the formation of salt due to the transfer of carboxylic acid proton to the N-atom of Acr.

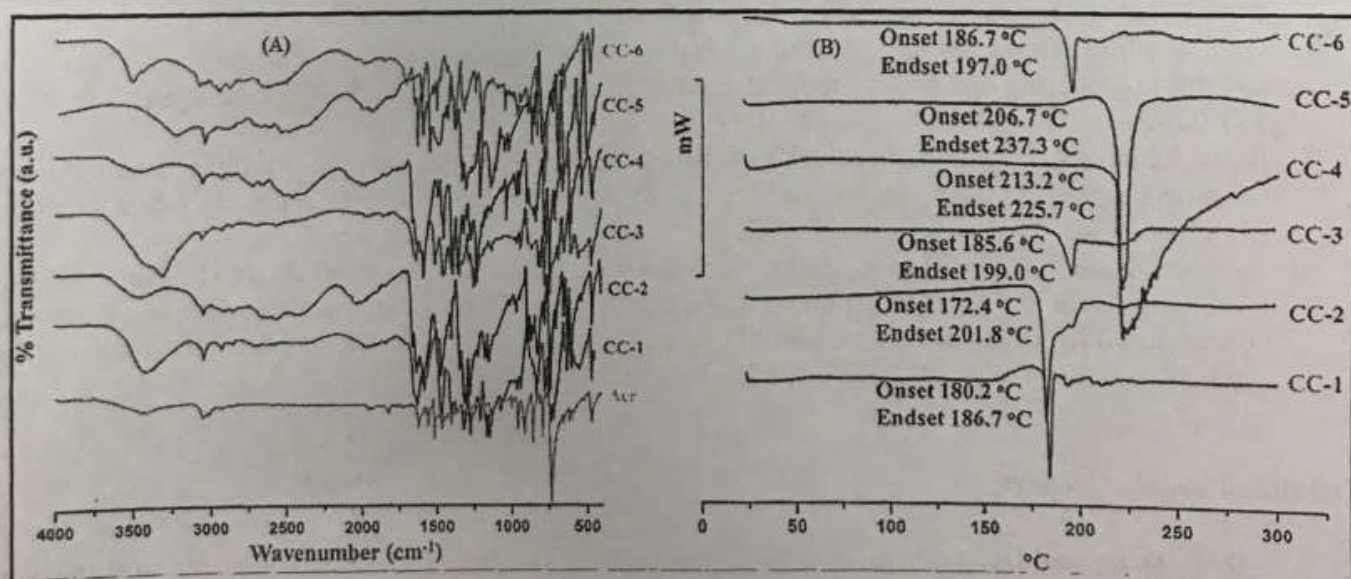


Figure 1: (A) FT-IR spectra of Acridine co-crystal/salt with isomeric dihydroxybenzoic acids (CC-1 to CC-6) compared with pure Acridine; (B) DSC endotherms represent melting onset & end set of the co-crystal/salt CC-1 to CC-6.

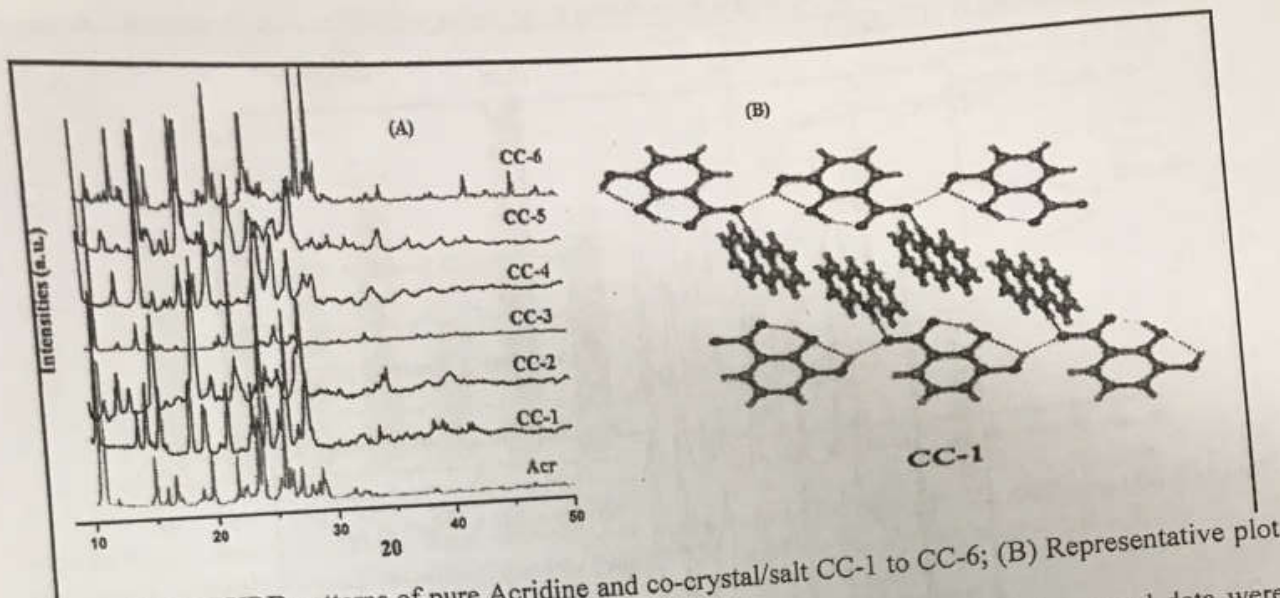


Figure 2: (A) PXRD patterns of pure Acridine and co-crystal/salt CC-1 to CC-6; (B) Representative plot of molecular packing of CC-1. The guest-free crystalline modification of CC-1 was isolated from ethanol and single crystal data were solved and refined in triclinic $P\bar{1}$ space group with one Acr and one 2,3-DHBA symmetry independent molecules. The crystal structure reveals the formation of salt as the carboxylic acid proton is transferred to the N of Acridine. The 2,3-dihydroxy benzoates form a molecular tape via O-H...O hydrogen bonds along the [100] axis. Protonated acridine is perpendicular to this molecular tape through N⁺-H...O⁻ hydrogen bonds. Two such molecular tapes intercalate each other through π ... π stacking of acridine and completing a sheet-like structure (Figure 2B). They are further arranged via C-H... π and C-H...O interactions to complete 2D packing. Such 2D molecular sheets are arranged via C-H... π to complete 3D packing of molecules. Thus, weak interactions like π ... π , C-H... π , and C-H...O interactions show significant roles in predicting the molecular arrangement in the lattice. Similarly, the observed SCXRD data for CC-1 to CC-4 and CC-6 are summarized in Table 1.

Table 1: Crystallographic Parameters of Acridine Co-crystal/Salt Materials CC-1 to CC-4 and CC-6

Crystal data	CC-1	CC-2	CC-3	CC-4	CC-6
Formula unit	C ₂₀ H ₁₅ NO ₄	C ₂₀ H ₁₄ NO ₄	C ₂₀ H ₁₅ NO ₄	C ₂₀ H ₁₅ NO ₄	C ₄₆ H ₃₃ N ₃ O ₄
Formula wt.	333.33	333.33	333.33	333.33	691.75
Crystal system	triclinic	monoclinic	triclinic	monoclinic	monoclinic
a [Å]	7.5239 (13)	7.6721 (8)	7.1782 (4)	7.4299 (2)	15.604 (10)
b [Å]	9.4723 (17)	9.6531 (9)	8.7005 (6)	23.1999 (8)	14.4410 (9)
c [Å]	11.580 (2)	21.693 (3)	13.4602 (10)	9.6852 (3)	16.911 (11)
α [°]	108.045 (8)	90	73.908 (6)	90	90
β [°]	93.572 (9)	95.218 (7)	74.603 (4)	101.105 (2)	106.39 (7)
γ [°]	90.94 (2)	90	87.739(4)	90	90
Volume [Å ³]	782.6 (2)	1599.9 (3)	778.19 (9)	1638.21 (9)	3656 (4)
Space group	$P\bar{1}$	$P21/n$	$P\bar{1}$	$P21/c$	$P21/c$

In order to understand the pharmacokinetic properties of all six cocrystals/salts, we further performed phase stability, solubility and permeability studies under physiological condition using different spectroscopic techniques. A parallel set of slurry experiments was carried out at pH 1.2 and pH 7.4. The

Basim Samir

materials retrieved from these experiments were found to be stable upto 12 h. A representative example of CC-1 is demonstrated in Figure 3.

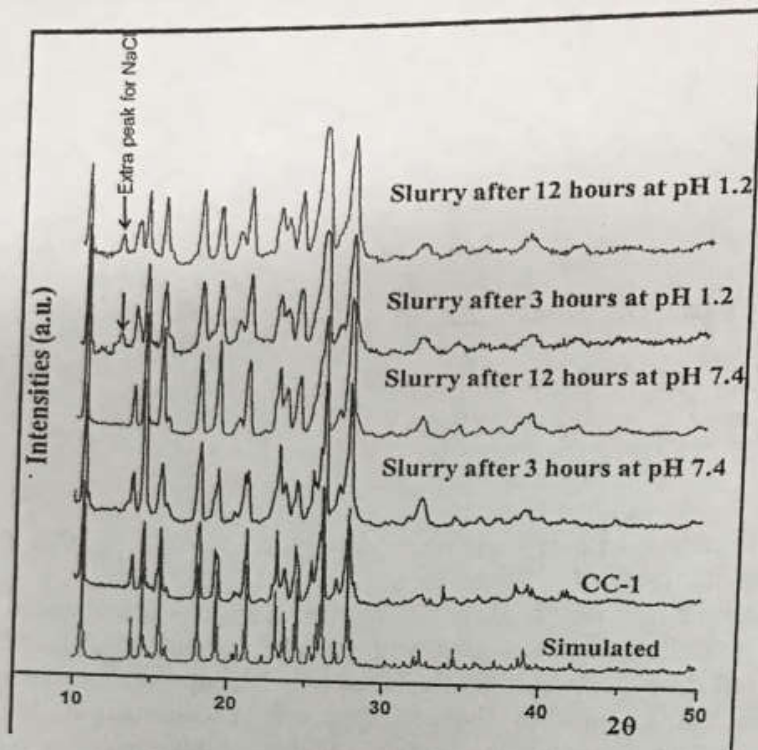


Figure 3: Phase stability test of CC-1 confirms (by slurry experiment) its stability by the obtainment of identical PXRD patterns at pH 1.2 and 7.4 up to not less than 12 h.

As desired solubility and permeability factors were determined for powder materials at pH 1.2 and pH 7.4. The representative results are demonstrated in Figure 4A-4B. The solubility of materials in acidic pH depends on acidity of the cofomers. The stronger the acidity of cofomers, the higher will be its tendency to remain in ionized form in acidic medium. Hence, the ionic salt tries to retain its ionic form at pH 1.2 resulting in lower solubility in polar media. Similarly, permeability studies suggested the better $\pi \cdots \pi$ off-stacking which is responsible for better thermodynamic stability and slower rate of permeation. The outcome of physiochemical property studies of multicomponent crystals of small molecules allowed us to establish a link of its properties to adhesive and cohesive intermolecular forces such as hydrogen bonds and most importantly $\pi \cdots \pi$ interactions. Essentially this study demonstrated how these non-covalent interactions especially $\pi \cdots \pi$ interactions play a crucial role in modifying molecular packing energies in the multicomponent drug formulation. A schematic representation of Acr-DHBA drug cocrystals/salt is shown in Figure 5.

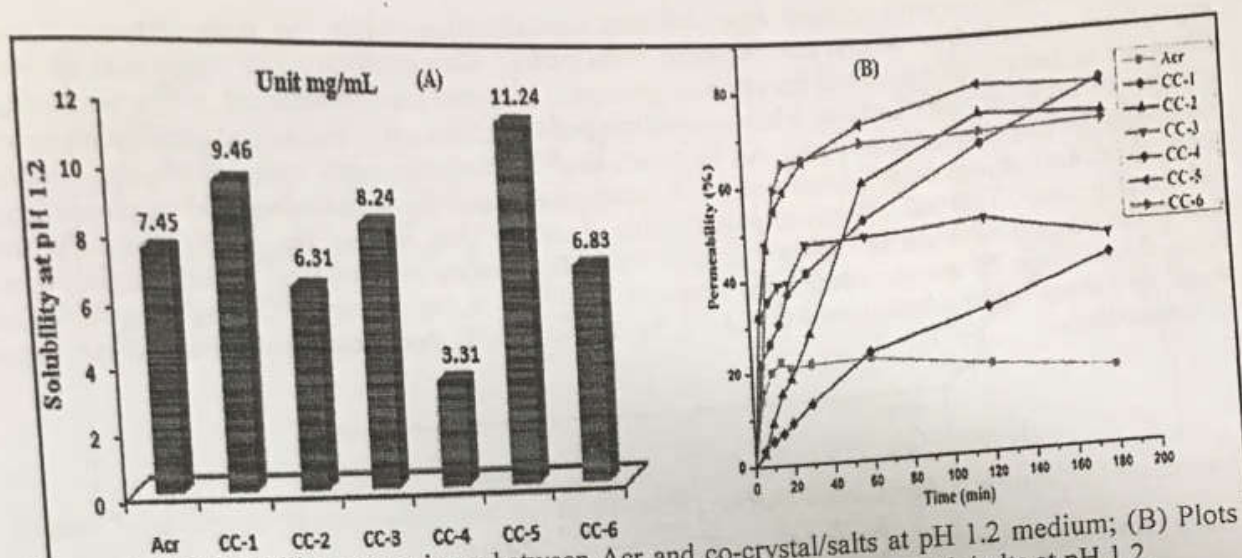


Figure 4: (A) Solubility comparisons between Acr and co-crystal/salts at pH 1.2 medium; (B) Plots of membrane permeability profiles with respect to time of Acr and their co-crystals/salts at pH 1.2.

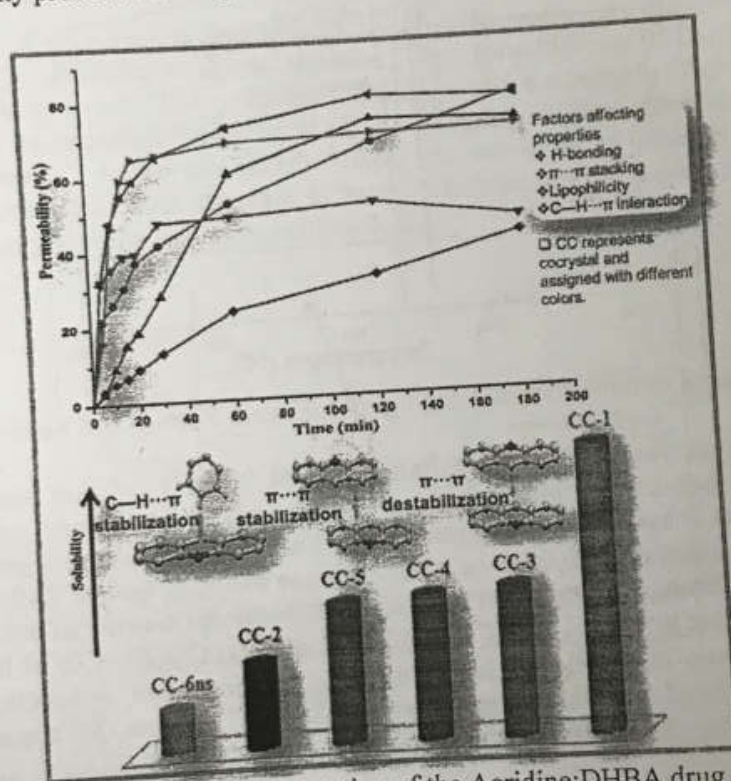


Figure 5: Schematic representation of the Acridine:DHBA drug cocrystal.

3. Trimorphic ethenzamide cocrystal: in-vitro solubility and membrane efflux studies:

In this system, we were successful to generate three distinct forms of ZMD-2,4-DHBA cocrystals (Form-I, Form-II, and Form-III). The present study will focus on understanding solubility and membrane permeation behaviour that can have an acute effect on the efficacy of the drug in their various cocrystal polymorphic phases. An equimolar mixture of ZMD and 2,4-DHBA (1:1) was taken in a mortar and pestle and ground for about 2 h in the presence of a few drops of acetonitrile. The grinded material was left for crystallization from solvent with or without adding formic acid as additive. Both crystallization conditions at room temperature afforded block type colourless crystals of Form-I. The Form-II of

Bijul Sarma

ZMD-2,4-DHBA cocrystal appears from solution crystallization, while the molar ratio is 2:1 and crystallizes out only from formic acid (crystallization media). Slow evaporation of formic acid afforded a fibre-like material of Form-II, and therefore single crystal data could not be obtained. A few block-shaped crystals of Form-III were isolated while crystallizing out concomitantly and serendipitously along with Form-I in the presence of formic acid. All forms are characterized thoroughly and serendipitously along with various spectroscopic techniques and subjected for solubility and cell membrane permeability studies at different physiological pH environments. Thermal analysis of polymorphic phases by DSC renders new solid phase differ from that of the starting materials as well as from each other. The melting onset on DSC endotherm for Form-I, Form-II and Form-III are recorded in the range of 30-300 °C at the rate of 3 °C min⁻¹ (Figure 6). The single and sharp melting endotherms at 118 °C, 92 °C and 111 °C represents Form-I, Form-II and Form-III respectively.

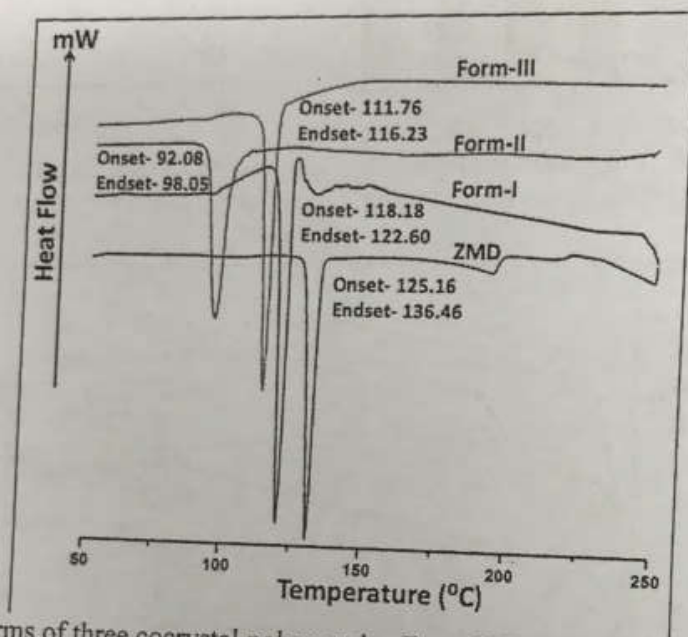


Figure 6: DSC endotherms of three cocrystal polymorphs, Form-I, Form-II and Form-III.

Similarly, other techniques like FT-IR, PXRD, Raman spectra SCXRD etc were used to characterize the formation of cocrystal polymorph. Interestingly, SCXRD analysis for Form-I and Form-III firmly confirmed the differences in hydrogen bond synthons essentially the molecular arrangement of the lattice. Form-I crystallizes in monoclinic $P21/n$ space group with one molecule each of ZMD and 2,4-DHBA in the asymmetric unit. The molecule 2,4-DHBA is resolved its positional disorder of ortho-OH group in the ratio 70:30 (%) with respect to COOH group. The structure displays COOH...COOH homo synthon with $R_2^2(8)$ dimer motif (Figure 7a) through O-H...O hydrogen bonding. Here, ortho-OH apparently forms intramolecular hydrogen bond with the oxygen atom of COOH. The para-OH connects ZMD via O-H...O and O...H-N synthons (Figure 7a-7b).

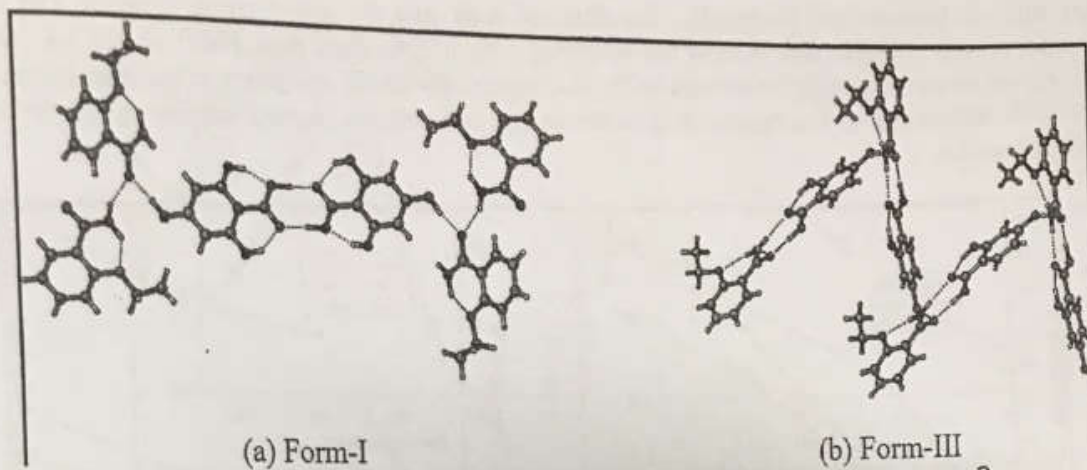


Figure 7: (a) Crystal structure of Form-I displays COOH...COOH homo synthon with $R_2^2(8)$ dimer motif. (b) Form-III consists of COOH...CONH₂ heterosynthon with similar $R_2^2(8)$ hydrogen bonded dimer motif.

The solubility studies of ethenzamide and their cocrystal polymorphs were examined at pH 1.2 and 7.4 (Figure 8). Interestingly, solubility parameter signifies higher solubility rate of ZMD at pH 1.2 due to the formation of hydrochloride salt. The protonated ZMD formed a strong hydrogen bond with solvent molecules enhancing its solubility. However, at pH 7.4 phosphate buffers, the solubility of both Form-I and Form-II increases 2.5 times than ZMD. Since, the solubility is inversely related to melting temperature of the cocrystal. Thus, decrease in melting temperature of the drug *via* cocrystallization lowers the lattice energy, thereby leading to better solubility.

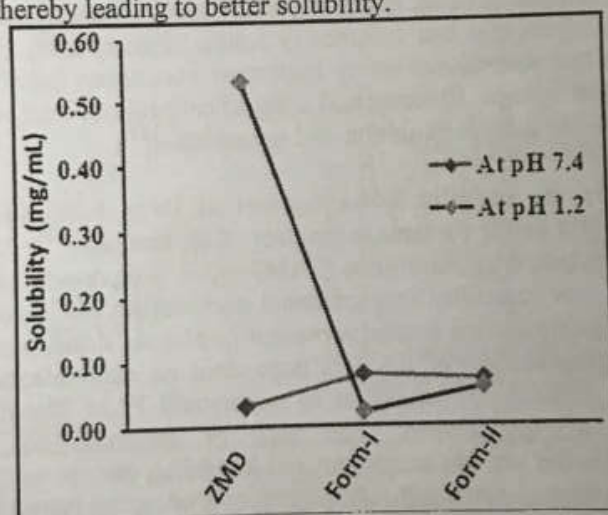


Figure 8: Solubility of Ethenzamide and its cocrystal polymorphs, Form-I and Form-II at pH 1.2 and pH 7.4 conditions.

The overall bioavailability study is triggered by permeability and diffusion behavior of the drug materials and therefore we further evaluated these parameters for Form-I and Form-II and compared their studies with the parent drug molecule (Figure 9). The results demonstrated that the permeation rate of Form-I (~23%) is approximately three times higher than that of ZMD (~7%) at 30 min under pH 7.4. Formation of hydrochloride salt would be the reason for better interactions with solvent media and therefore it lowers the initial permeation rate for pure ZMD at this pH condition. At pH 1.2, permeation rate of Form-I is higher than that of ZMD (upto 30 min). This is because of the formation of cocrystal between the drug and coformer leaves fewer sites for hydrophilic interactions from solvent molecules which causes in

Bipin Sanyal

higher rate of permeation. Eventually, the flux of drug and its polymorphs (Form-I and Form-II) calculated revealed higher flux density for cocrystal polymorphs than pure ZMD at pH 7.4. At pH 1.2 solutions, we observed similar improvement in flux density for ZMD and Form-I, whereas it remains low for Form-II influenced by the exposure of polar groups towards the crystal surface to interact with the solvent molecules.

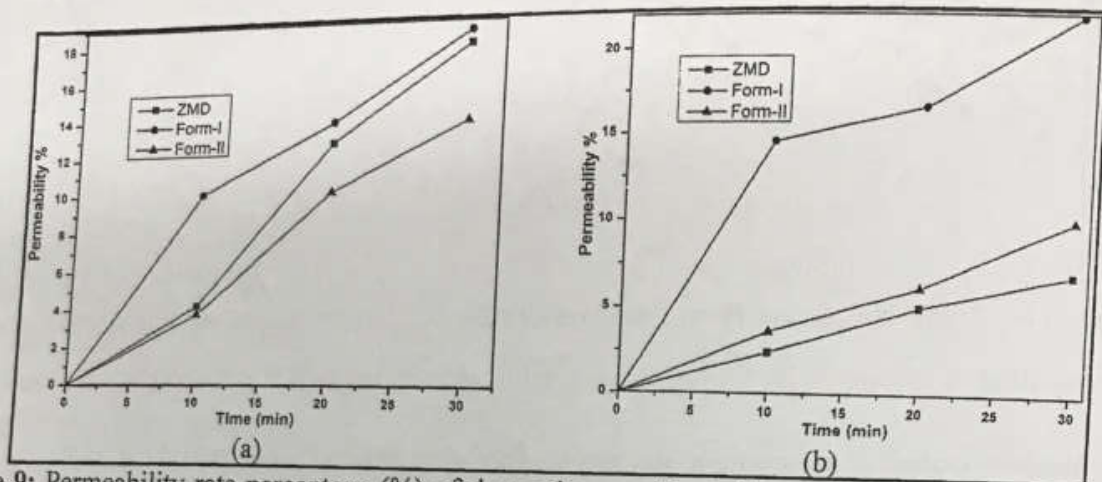


Figure 9: Permeability rate percentage (%) of drug ethenzamide and its cocrystal polymorphs, Form-I, Form-II, Form-II (a) at pH 1.2 and at PH 7.4 conditions.

Here we reported a system with better physical and chemical properties based on solute-solvent interactions, molecular symmetry, hydrogen bond synthons and particle size distribution. Phase stability of polymorphic phases was monitored by slurry experiment. Atmospheric stability was examined using dynamic vapor sorption analysis that had satisfactory results. Present study on ZMD is the first kind of example where we examined several extremely important parameters between polymorphic phases of ZMD cocrystal. The present system demonstrated a significant role to improve drug bioavailability and appended an important note for drug formulation and optimization.

4. Mechanistic Study on Stability Enhancement of Drug Famotidine by Cocrystallization: Structure-Activity, Stability and Pharmacokinetics Correlations: In this work, we had taken histamine H_2 -receptor antagonist drug famotidine (FAM) which is reportedly categorized as BCS class IV drug due to its extremely low solubility and intestinal permeability. It is apparently an unstable drug corroborated after detecting degradation products present in plasma, urine, parental nutrient solution and gastrointestinal tract. The degradation of FAM is dependent on experimental pH conditions. We had chosen physiological i.e., stomach pH condition to understand FAM degradation behaviour where it showed maximum rate of degradation. The rate of decomposition of famotidine studied spectrophotometrically under the present condition by monitoring the absorption (A_{obs}) of famotidine at 286 nm as a function of reaction time (t) following the equation i.e., $[\ln[A_t]/[A_0] = -kt]$; Where $[A_0]$ and $[A_t]$ are the absorbance at zero and "t" time respectively. The rate constant (k) for famotidine is found to be $4.93 \times 10^{-3} \text{ min}^{-1}$ (Figure 10B). The change in absorption spectra of famotidine at 1.2 pH conditions with time have been monitored and given in Figure 10A.

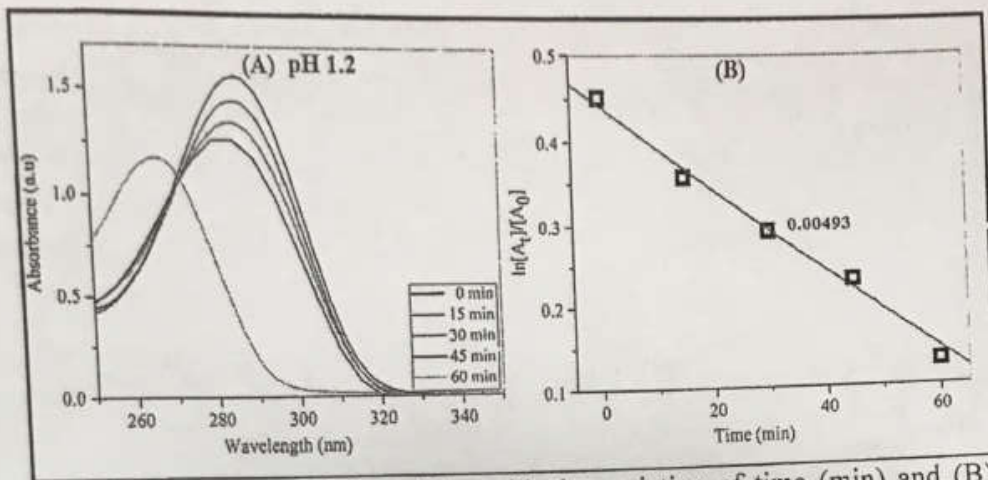


Figure 10: (A) Absorption spectra of famotidine with the variation of time (min) and (B) Plot of $\ln[A_t]/[A_0]$ vs. time required during hydrolysis under pH 1.2 conditions.

The degraded product (D-FAM) of FAM was analyzed by using different spectroscopic techniques. The entirely different FT-IR spectra of FAM and D-FAM (Figure 11A) indicate the phase transformation of famotidine at pH 1.2. The absorption peak that appears at 3383 cm^{-1} is attributed to the N-H stretching vibration of the primary amide of the decomposed material. Further, a new peak at 1686 cm^{-1} also indicates the generation of C=O group for the decomposed material. PXRD pattern of D-FAM (Figure 11B) exhibits difference in some of the major peak positions and pattern of intensities from that of pure famotidine.

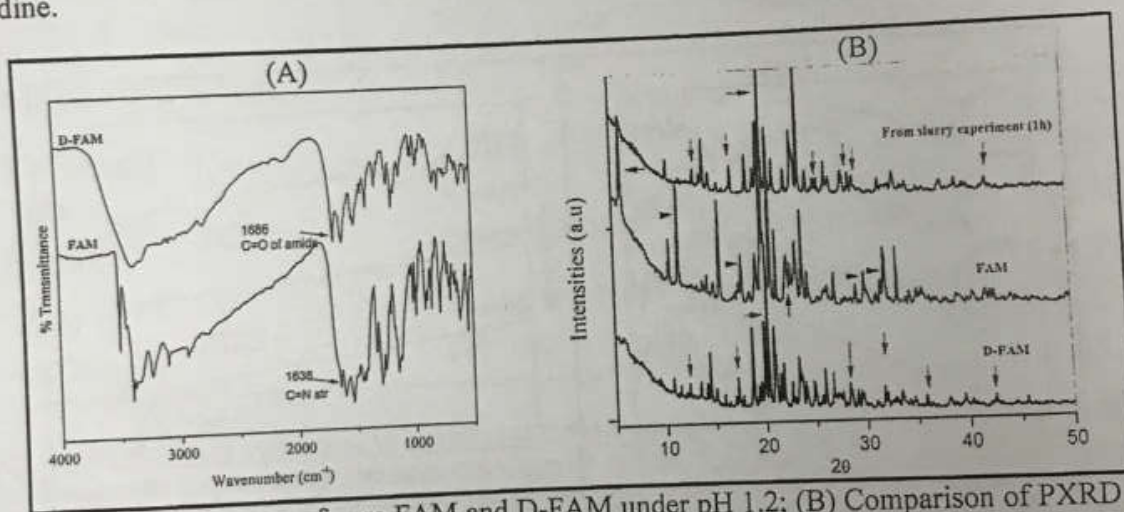
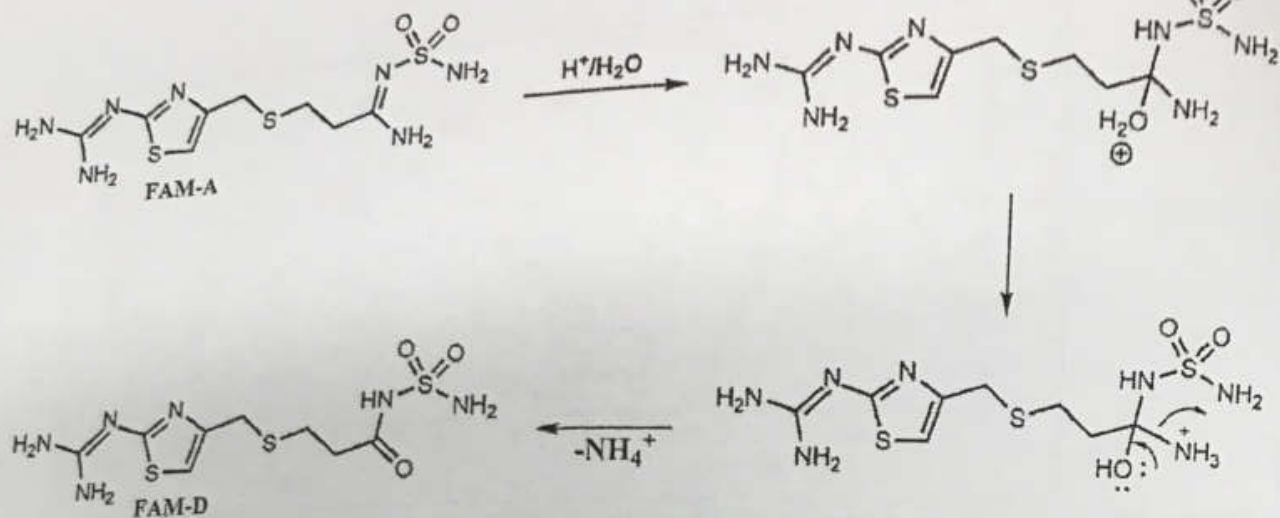


Figure 11: (A) FT-IR spectra of pure FAM and D-FAM under pH 1.2; (B) Comparison of PXRD patterns of pure famotidine, D-FAM and the material obtained from the slurry experiment at pH 1.2

After analyzing the D-FAM material, we propose a mechanistic pathway for the hydrolysis of famotidine that involves the following basic steps as shown in Scheme 1.

Bijul Sarma



Scheme 1: Plausible mechanistic pathways of famotidine degradation at pH 1.2

After deliberate examination of famotidine decomposition at different experimental conditions and identifying its relative decomposition site, cocrystallization technique is explored to prevent FAM degradation. The xanthine cofomers such as theophylline, caffeine, and theobromine also exhibit complementary hydrogen bonding sites. Thus, the formation of cocrystals is predictable based on the probability of different heterosynthons formation. Accordingly, liquid-assisted mechanochemical grinding method is used to synthesize three different cocrystals of famotidine. The synthesized cocrystals are characterized by using FT-IR, PXRD, DSC and SCXRD techniques. Representative spectra of FT-IR and DSC endotherms are shown in Figure 12.

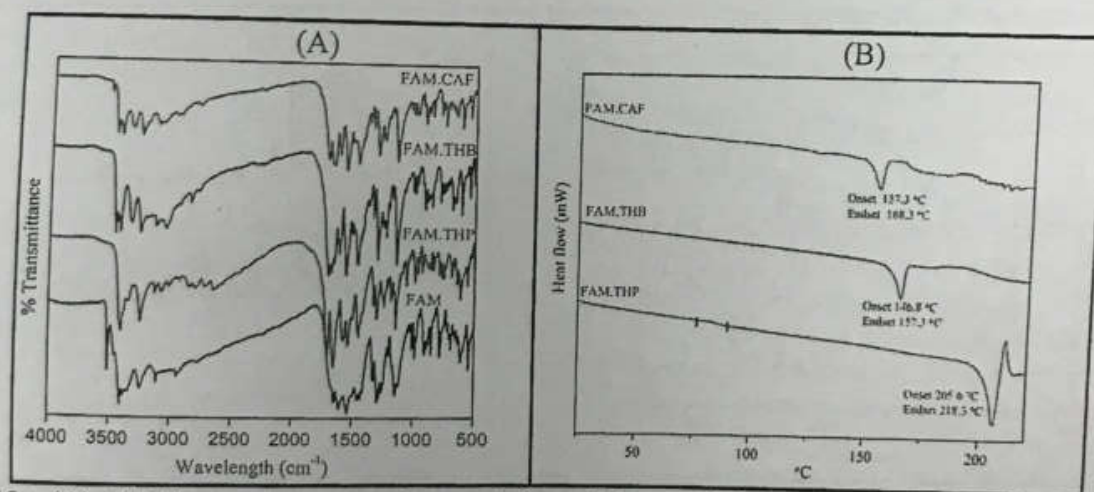


Figure 12: (A) FT-IR spectra comparison of famotidine and its cocrystals; (B) DSC endotherms representing the melting onset temperature of famotidine cocrystals

FAM·THP is crystallized out from methanol and solved with the triclinic space group $P\bar{1}$. The asymmetric unit consists of one molecule of FAM and two molecules of THP (Figure 13). The unit cell parameters are given in Table 2.

Table 2: Single crystal X-ray data parameters of FAM and FAM.THP

Crystal data	FAM·THP	FAM Form A
Formula unit	$C_{22}H_{31}N_{15}O_6S_3$	$C_8H_{15}N_7O_2S_3$
Formula wt.	697.80	337.45
Crystal system	Triclinic	Monoclinic
T [K]	296	296
a [Å]	7.7722(6)	12.0082(4)
b [Å]	13.4252(10)	7.2103(4)
c [Å]	14.6013(11)	16.8488(8)
α [°]	98.375(4)	90
β [°]	92.445(5)	99.807(3)
γ [°]	93.659(5)	90
Volume [Å ³]	1502.1(2)	1437.50(12)
Space group	$P\bar{1}$	$P2_1/c$
Z	2	4
D_{calc} [g cm ⁻³]	1.543	1.559
μ (mm ⁻¹)	0.314	0.529
Reflns. collected	7611	3642
Unique observed	4555	2762
R1 [I > σ (I)]	0.0519	0.0390
wR2	0.1690	0.1320
Instrument	Bruker APEX-II	Bruker APEX-II
X-ray	Mok α ; $\lambda=0.71073$	Mok α ; $\lambda=0.71073$
CCDC no.	1891140	1891137

A slurry experiment was performed to examine the phase stability of famotidine and its cocrystals at pH 1.2. Solid materials that are extracted from the slurry at certain time intervals are characterized by PXRD. The PXRD patterns of solid cocrystal material of FAM·THP, retrieved from slurry retain the original peak position even after 24 h. It has confirmed the phase stability of this cocrystal material at pH 1.2. However, there are significant phase changes observed in PXRD patterns of famotidine recovered from slurry within 1 h, which is due to the formation of D-FAM. Stacked PXRD plots obtained from the slurry of drug famotidine and cocrystal FAM·THP at different time intervals is shown in Figure 14.

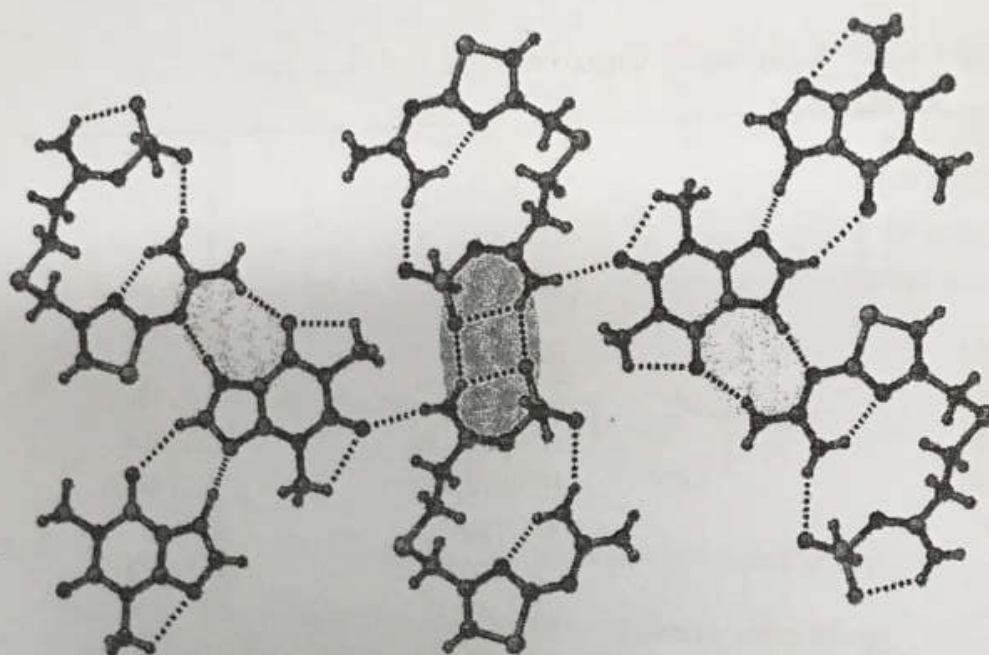


Figure 13: $R_2^2(12)$ homodimer (red circle) and $R_2^2(9)$ heterodimer (blue circle) involved in the formation of FAM·THP

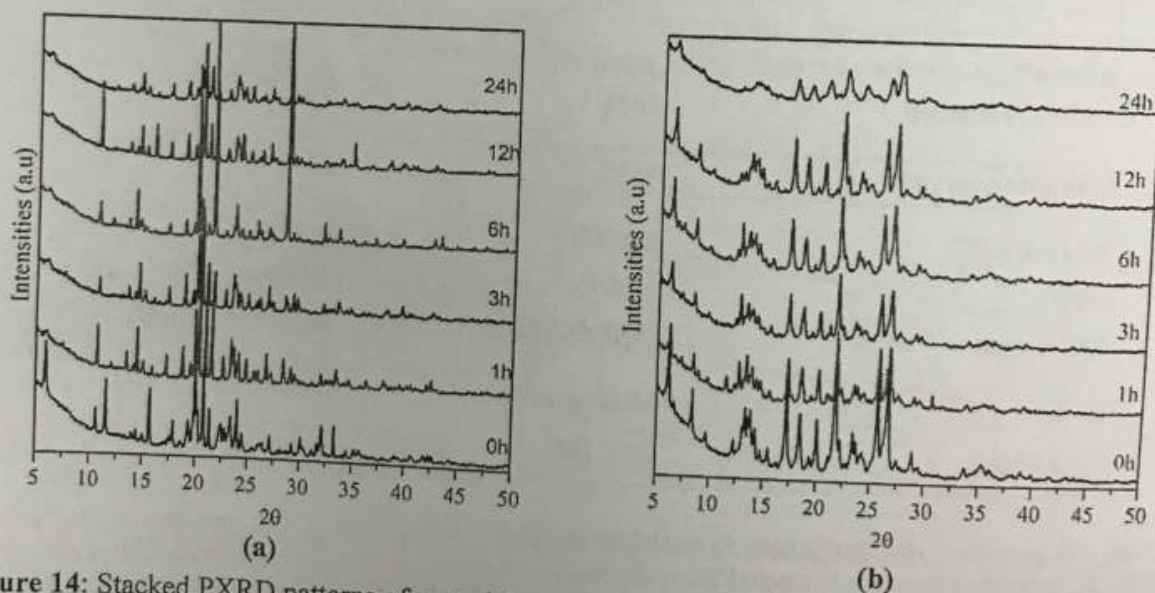


Figure 14: Stacked PXRD patterns of materials obtained from slurry experiments at pH 1.2 up to 24h (a) FAM and (b) cocrystal FAM·THP.

In highly acidic condition, the $-C=N$ site of the amidine group of FAM-A is susceptible to hydrolysis. The hydrolysis product is the isolated FAM-D. The improved stability of the FAM·THP cocrystal under similar pH environments is attributed to the involvement of strong heterosynthons, i.e. $N-H\cdots N$, $C-H\cdots O$, and $N-H\cdots O$ hydrogen bonds. Indeed, the use of xanthine base cofomers offers such strong heterosynthons which easily change the molecular conformation of the drug FAM-A at different torsion angles (ϕ). A list of the measured changes in torsion angle for the famotidine molecule in FAM-A and FAM·THP cocrystal is given in Table 3.

Table 3: Torsion Angles (ϕ°) in molecular conformers of FAM-A and FAM·THP

Molecular conformer	Torsion angle (ϕ°)	
	FAM-A	FAM·THP
C12-C11-S10-C9	106.92	69.87
C11-S10-C9-C8	90.26	63.90
S10-C9-C8-C6 (ϕ_1)	68.77	178.36
C9-C8-C6-N7 (ϕ_2)	101.00	86.99
C9-C8-C6-N5	77.01	86.56
C8-C6-N7-N5	2.27	179.52
C8-C6-N3-S3 (ϕ_3)	175.38	75.67
C6-N7-N5-S3	4.27	0.67
C6-N5-S3-N1	120.72	75.67

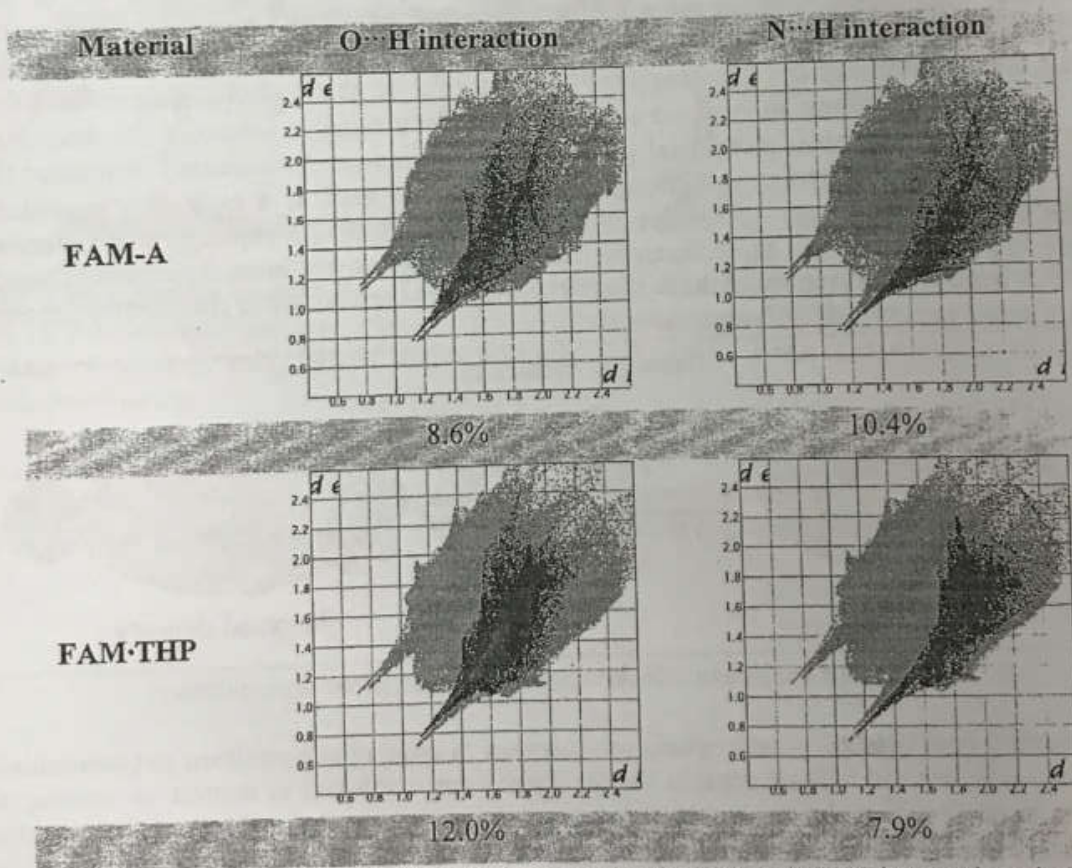
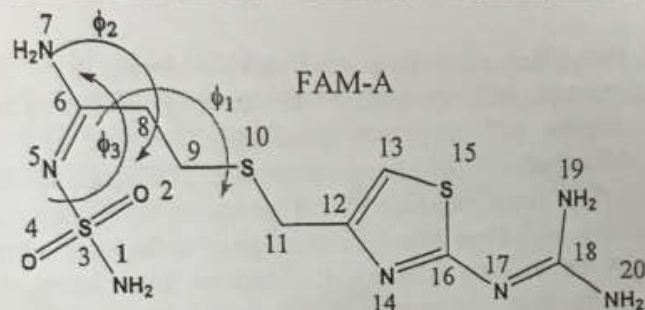


Figure 15: Comparison of Hirshfeld surfaces analysis of O...H and N...H interactions in FAM-A and FAM·THP cocrystal

The change in torsion angle of FAM-A in FAM·THP cocrystal at ϕ_1 (S10-C9-C8-C6), ϕ_2 (C9-C8-C6-N7), and ϕ_3 (C8-C6-N3-S3) signifies clear differences in the orientation of their

Samy

functionalities from pure FAM-A conformation. Thus, it allows the FAM-A molecule to keep the $-C=N$ site buried inside. Auxiliary support in strengthening the molecular packing has been offered by $N-H\cdots N$ and $N-H\cdots O$ inter- and intramolecular hydrogen bonding in cocrystals. In turn, this situation directs the solid toward hydrolysis on the amidine group of the $-C=N$ site. The Hirshfeld surface area analysis is performed to quantify the intermolecular interaction that is present in the synthesized cocrystal and compared with that of pure FAM-A (Figure 15). It is interesting to note that the contribution of the $O\cdots H$ interaction is 8.6% for FAM-A, which is further increased to 12.0% for the FAM·THP cocrystal. A higher contribution of the $O\cdots H$ interactions advocates for stronger interaction possibilities. In parallel, the contribution of a weaker $N\cdots H$ interaction is also higher for FAM-A (10.4%) and drops down to 7.9% for FAM·THP. Perhaps compensation in the contribution of interactions offers a significant stability enhancement in the cocrystal. Thus, cocrystallization offers a viable route to stabilized drug degradation. Cocrystallization can be an efficient way to address the stability of drug molecules associated with the susceptibility of acid hydrolysis.

5. Nanocarriers in Drug Delivery: Eminence and Confront: In the pharmaceutical discipline, the search for pioneering drugs and delivery method to the targeted site is a major concern for disease management, due to the limited efficacy, poor bio-distribution, and lack of selectivity in the current treatment procedure. An estimated 40% of pharmaceutical ingredients acquired market approval and 90% of them have been suffering from solubility and permeability issues, in vivo stability, intestinal absorption, hasty metabolism, and even elimination of poor safety and admissibility. Recently, various researches in drug delivery have been intended to confront these issues through the development of nanostructure materials. It requires various scientific principles to develop materials in the field of pharmaceuticals, which could have extensive and paradigm shifting relevance for indispensable research on drug innovation and medical technology. In this case, nanocarriers have immense potential which lies in controlling the drug delivery and targeting drug release profile of pharmaceutical ingredients followed by different routes of administration. Various strategies have been using to formulate the drug carriers with the improvement of their physicochemical properties. It has increased the overall beneficial therapeutic index of new or active ingredients. Although nanocarriers are used as a promising candidate in drug delivery, some of the foremost pinnacles remained unanswered. To explore their potential ability, researchers have to address all those concerns before it comes to a clinical approach. Therefore, it is expected that the overall summary of these chapter will help the researches to standardize protocol for the detection of nanocarriers under development.

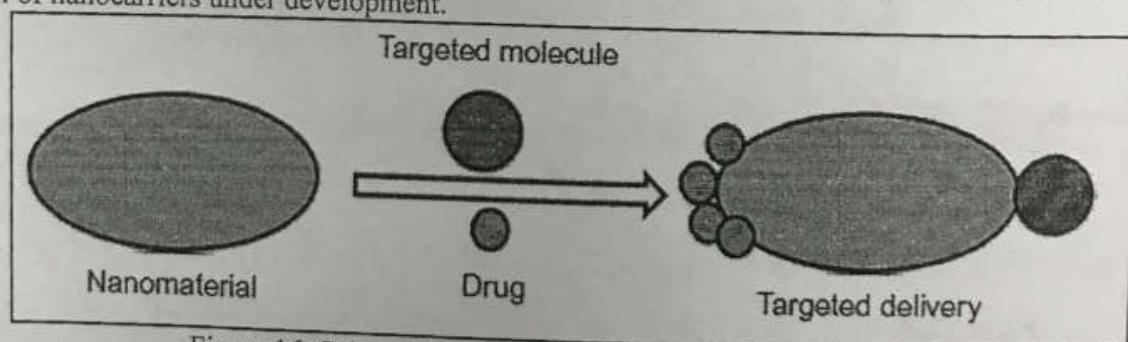


Figure 16: Schematic representation of targeted drug delivery.

6. Oriented crystallization on organic monolayers to control concomitant polymorphism: Self-assembled monolayers (SAMs) of organic thiols, silanes are employed to control nucleation, size and shape of the crystals with polymorph selectivity, an extremely important subject in the pharmaceutical development. The nucleation events and crystal growth can be guided by molecular recognition at the interface uttered by intermolecular interactions. Short-acting antimicrobial sulfa drug sulfathiazole is known for its concomitant crystallization with five existing polymorphs due to conformational flexibility and hydrogen bond synthon variation. The relative conformer energies (E_{conf}) are calculated using DFT, B3LYP/6-311G⁺⁺ (d,p) basis set with respect to the dihedral angle C2-C3-S14-N17. Further, packing

energies are calculated using "UNI" force-field popularized by Gavezzotti and Filippini. Packing energy suggests the increasing order of stabilization of the polymorphs, as $II < III < IV < V < I$. Stabilization energy analysis further suggests comparable packing energies for polymorph II, III and IV which offers SULF molecule to nucleate concomitantly.

Functional self-assembled monolayer (SAM) of organic thiol on gold surface has been employed as an efficient approach to control concomitant nucleation of such flexible drug and emphasized. Initially, interfacial properties such as wettability and contact angle of the prepared SAM surfaces was measured and the result showed the decreased in contact angles for different organic thiol-based gold surfaces (Figure 17). The morphology of bare surfaces was also analyzed using AFM and FESEM techniques. The crystallization on bare gold surfaces and the solution crystallization in gold surfaces afforded concomitant form I, II, IV and II, III, IV respectively which is further confirmed by PXRD analysis.

However, the functionalized gold surfaces offer variation in chemical functionality, molecular structure, and geometry of the surfactant monolayer and the crystals nucleates on functionalized surfaces were individually characterized using confocal Raman microscopy.

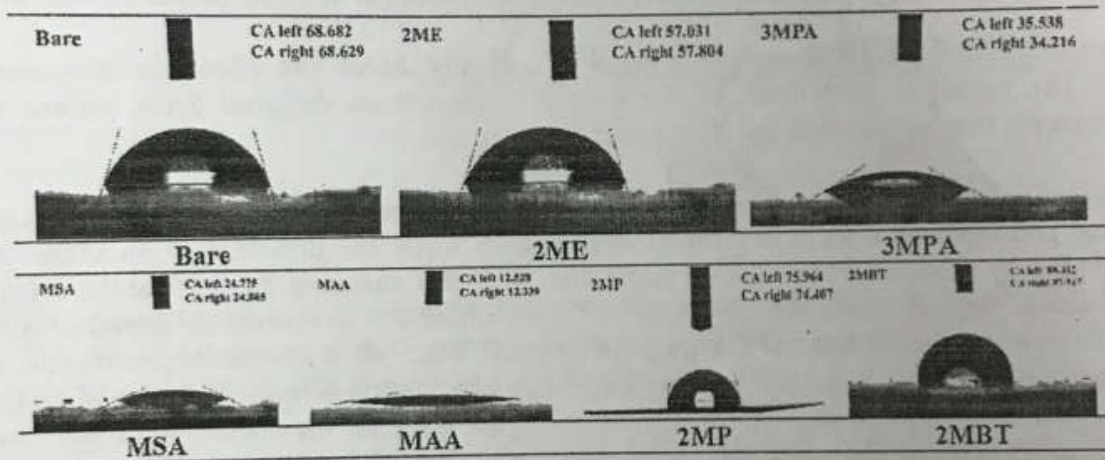


Figure 17: Contact angle comparison of water droplet onto different thiol functionalized SAM surfaces with that of the bare gold surface; where 2ME: 2-Mercaptoethanol, 3MPA: 3-Mercaptopropionic acid, MSA: Mercaptosuccinic acid, MAA: Mercaptoacetic acid, 2MP: 2-Mercaptopyridine and 2MBT: 2-Mercaptobenzothiazole.

Crystals appeared from solution crystallization and on bare gold surfaces of SULF are blocks, needles or plates. The crystal growth and habits of SULF are altered by SAM surfaces. Optical microscopy images of crystals showing different crystal habits of SULF obtained on respective SAM surfaces (Figure 18).

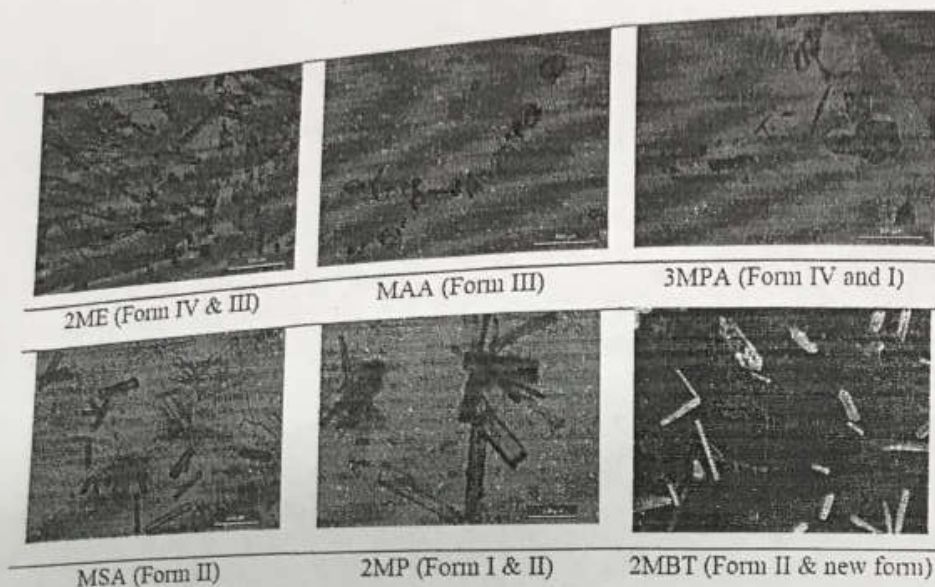
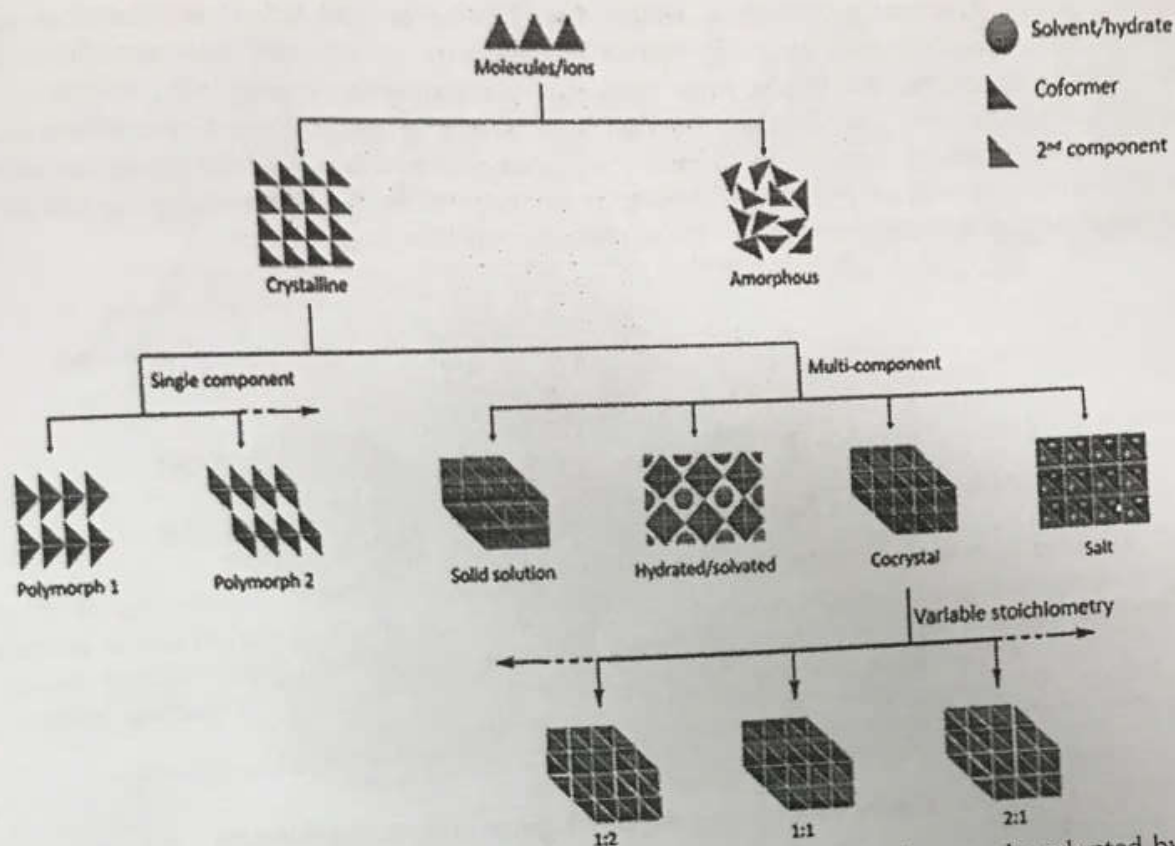


Figure 18: Optical microscopic images of different crystal habits of SULF observed on SAM surfaces.

The crystallization on SAM surface is mostly kinetically driven and often nucleates novel metastable forms. The unknown sixth form of the drug is nucleated on designed SAM surface supported by spectroscopy, thermal analysis and X-ray diffraction studies.

In conclusion, nucleation of pure polymorphic phase of highly concomitant drug like sulfathiazole is achieved and reported with pure form III nucleated on MAA and pure form II on MSA SAMs. This is conceivable by designing selective crystallization of SULF changing the preferential orientation of the crystal facets. An infrequent Raman spectrum for a peculiar fine needle crystal appeared on 2MBT SAM reveals a new metastable form of the drug and reported. These observations suggest that the translation of the structural information through the interface occurs by stereo chemical registry and functional groups in the SAM that play the role of an oriented surrogate layer for the nucleating crystal and control the crystallization process. Certainly, this study opens up opportunities of nucleating selective polymorphs of active pharmaceutical ingredients that often presents challenges.

7. Variable stoichiometry cocrystals: occurrence and significance: The occurrence of variable stoichiometry cocrystals offers the prospect to acquire more solid forms of the same system. The control of stoichiometry is extremely important concerning purity and intellectual property (IP) protection. We have analyzed structures, synthetic methodologies and properties of the reported variable stoichiometry organic cocrystals reported in the last decade, with discussion of their controlled production for drug formulation plans. This review further fetches an understanding of the accountable reasons for the existence of stoichiometry variation in cocrystals, which essentially results from the disparity in properties with IP coverage.



Scheme 2: Pictorial representation showing the most probable solid forms that can be adopted by a drug candidate. The few most common stoichiometry variations, viz. 1:2, 1:1 and 2:1, in cocrystals are displayed. The dotted arrow signifies the existence of more possible forms.

Nonstoichiometric compounds are generally associated with structural deformations and that too is controlled by the thermodynamic regime. In the last two decades, cocrystallization has emerged as a tangible way of fine-tuning different physicochemical properties of active molecules with a unique attention on pharmaceutical ingredients. Different stoichiometry cocrystals are an aspect of cocrystallization which can offer various new solid forms of an API with intellectual protection. Though there are a considerable number of cocrystal reports coming out every day, the number of different stoichiometry cocrystals is not high. We have summarized examples of different stoichiometry cocrystals reported mostly in the last decade with an emphasis on understanding the factors that can influence the formation of such different stoichiometry cocrystals, an imperative issue in the drug development process. The effects of solvents and coformer concentration on cocrystal stability have been highlighted. The variation of the physicochemical properties with different stoichiometry cocrystals is discussed. The number of representative examples in a distinct category is still limited, more exploration for accurate understanding and prediction of the structure-activity relationships in different stoichiometry cocrystals are necessary to recognize the stoichiometry of cocrystals from a formulation perspective.

8. Crystal engineering and pharmaceutical crystallization: This book chapter is a complete summary from the molecular sciences to industrial bulk sciences in the field of pharma cocrystals. From the inception of supramolecular chemistry to the propagation of crystal engineering in the solid-state pharmaceutical arena, the addition of new and better systems is listed and discussed thoroughly. The emergence of pharma cocrystals as a therapeutic entity calls for more extensive and rigorous scientific investments to study the effect of different crystallization parameters including stoichiometry, solvent, nucleation studies etc. The use of supramolecular gels, self-assembled monolayers, surface mounted

Bipul Sen

metal organic frameworks to influence nucleation and growth of crystalline phases are exemplified with emphasis on the structural and physicochemical amplification or modulations introduced as such. The application of such novel materials is highlighted with focus on the industrial scale manufacturing which often fails to regenerate the results from laboratory. Crystallization events, viz., nucleation, crystal growth, and polymorphic transformation are vital steps for quality end product. A comparison of the two methods of operation viz. batch operation and continuous operation is carried out listing out all the pros and cons associated with the processes. However, to bring down the cost of manufacturing it is found that continuous process manufacturing to be a better alternative for the pharma sector.

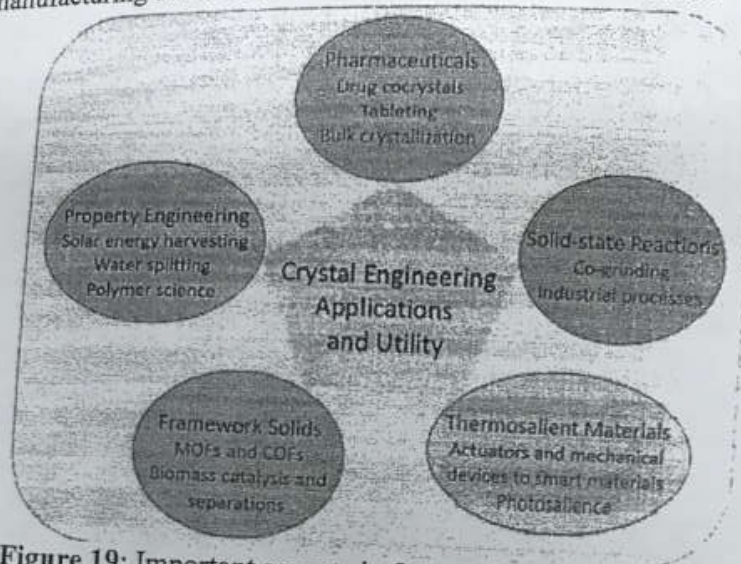
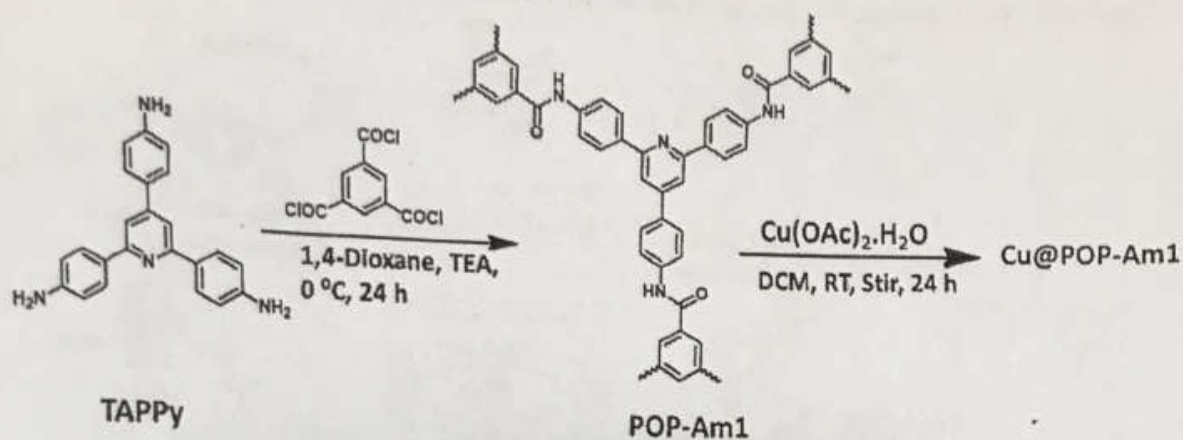


Figure 19: Important aspects in future of crystal engineering

9. Multicomponent Crystalline Solids: A Pre-Formulation to Discover Alternate Combination

Drug: The use of multicomponent solids such as salts, cocrystals, hydrates/solvates, mesoporous composites, co-amorphous solids, eutectic mixtures etc. It provides a platform to design and develop a drug with better therapeutic characteristics. Introduction of regulatory guidelines and patent portfolios for manufacturing cocrystals as new drug made this technology a popular trend in the R&D sector of pharma industry. This cocrystal technology is a drug development strategy to modulate pharmacological behavior of existing drug without changing their structural integrity. The subject crystal engineering offers ample opportunity to play with intermolecular interactions between the target drug and the conformer we use to integrate in the cocrystal synthesis during pre-formulation process. This review confers the present scenario on recent progresses of multicomponent crystalline solids especially cocrystals in pharmaceutical developments with an emphasis of cooperative efforts to discover an alternate hybrid drug. Recent examples, new synthetic strategies, advanced structural characterization techniques and future of multicomponent crystals for healthcare department are important wedges in this review. It is anticipated that this article will guide various approaches intended for better understanding of new drug phases.

10. Cu(II) Complex onto a Pyridine-Based Porous Organic Polymer as a Heterogeneous Catalyst for Nitroarene Reduction: Detoxification of 4 nitrophenol (4NP) by conventional water treatment technique is of rising concern owing to its high chemical stability and resistivity towards microbial degradation. The reduction of 4NP and/or nitroarene does not proceed under ideal conditions in absence of a catalyst. Utilizing organic porous polymers as support matrix for catalytic reactions we designed and synthesized a new pyridine based two-dimensional porous organic polymer connected by carboxamide functionality (POP-Am1) acting as heterogeneous catalyst carrier.



Scheme 3: Schematic representation of POP-Am1 and Cu(II) loaded POP-Am1

The POP-Am1 loaded with Cu(II) (Cu@POP-Am1) displays excellent catalytic behavior for 4NP reduction to 4 aminophenol (4AP) in shortest reaction time and improved yield percentage (%) compared to those reported using precious and expensive metal supported POPs. The nitrogen adsorption and desorption isotherm at 77 K exposes the permanent porosity and rigidity of POP-Am1.

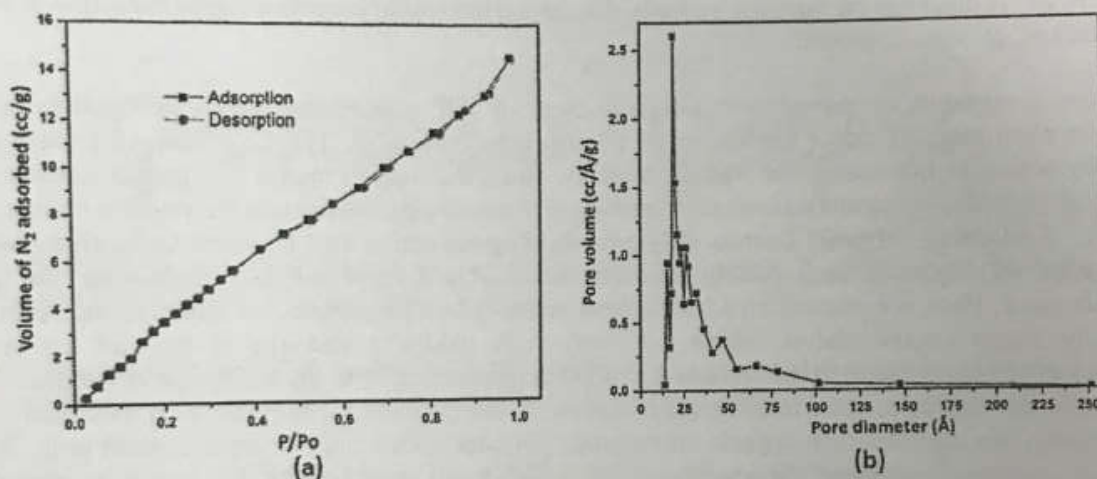


Figure 20: Nitrogen adsorption-desorption isotherm (a) and pore size distribution curve (b) of POP-Am1.

Figure 20a-20b displays the sorption curve and the pore size distribution. The lack in hysteresis of the isotherm signifies the reversible nature of nitrogen adsorption indicating identical adsorption-desorption mechanism. The Brunauer-Emmet-Teller (BET) surface area of POP-Am1 is calculated to be $27 \text{ m}^2 \text{ g}^{-1}$ and average pore diameter is 29.24 \AA affirms the polymer to be microporous in nature. Needless to mention that nitrogen containing ligand in coordination chemistry is well demonstrated as a versatile moiety to encapsulate or incorporate various metal ions. We opted for cheaper metals like copper to load onto POP-Am1. Obtained powder of copper loaded POP-Am1 (Cu@POP-Am1) was characterized by FT-IR, TGA, PXRD, EDS, AAS, ICP and TEM techniques. The isolated Cu@POP-Am1 was then subjected to investigate catalytic activity towards organic transformation reactions. As mentioned, for the reduction of 4-nitrophenol, we employed Cu@POP-Am1 as a catalyst for the reaction in presence of NaBH_4 . The addition of NaBH_4 acts not only as hydrogenating agent, but it also reduces Cu(II) to its metastable and/or unstable state in-situ. In the reaction, this reduced copper provides requisite electrons to 4-nitrophenolate and gets oxidize to stable Cu(II) species. The hydrogenating agent NaBH_4 then provide

Bijul Samra

the proton against the electron rich 4-nitrophenolate species and convert to 4AP eliminating water molecule. The complete catalytic cycle for conversion of 4NP to 4AP is depicted in Figure 21.

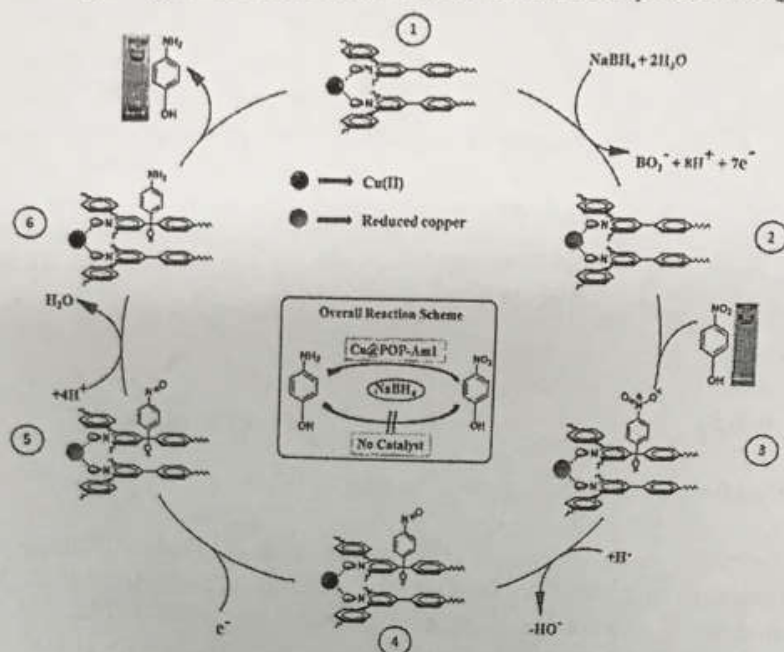
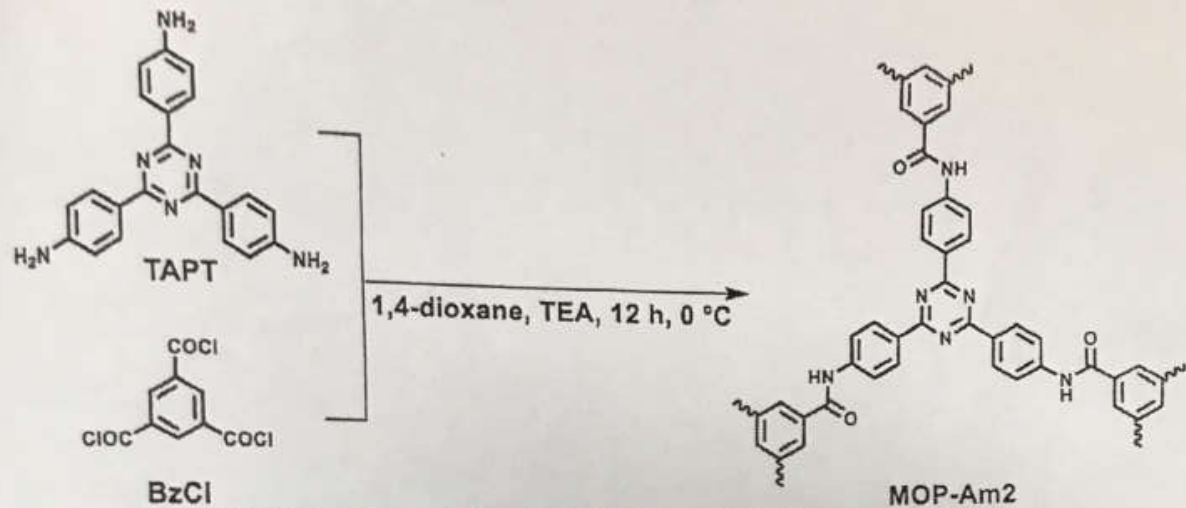


Figure 21: A plausible mechanistic pathway displaying the catalytic cycle towards reduction of 4-nitrophenol to 4-aminophenol.

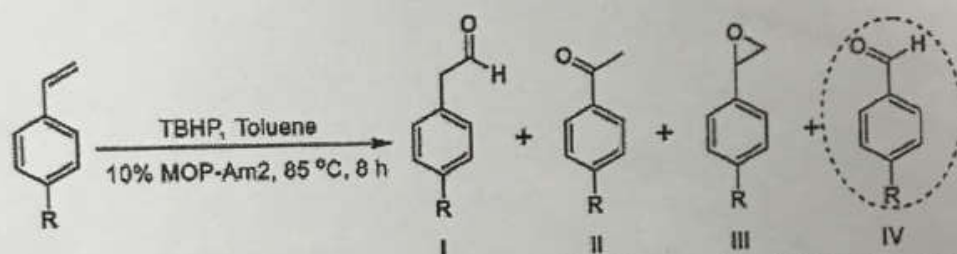
A close observation on the catalytic reduction cycle of 4NP with NaBH₄ describes the electron transfer rate between the BH₄⁻ donor and the respective acceptor molecules. The Cu@POP-Am1 plays a pivotal role by acting as intercessor for electron transfer. Thus, the support matrix i.e., porous organic polymer with continuous p-electrons and suitable functionality would play crucial role for electron transfer.

11. Endorsing Organic Porous Polymers in Regioselective and Unusual Oxidative C=C Bond Cleavage of Styrenes into Aldehydes and Anaerobic Benzyl Alcohol Oxidation via Hydride Elimination: Here, we pursued an advantageous pathway by designing a cost-effective and environment-friendly single organocatalyst, which can carry both oxidative cleavage of styrenes and anaerobic oxidation of benzyl alcohols self-reliantly in a single pot. Along with the highly active catalyst, it is also an important aspect to look into the regeneration of the catalyst. To perform such oxidative reactions effectively, we developed an organic mesoporous polymer with a high nitrogen content in it. The study reports a novel π -conjugated triazine-based POP (MOP-Am2) and identified it as one of its earliest metal-free organic catalysts, promoting the (i) oxidative cleavage of the C=C bond of styrenes in the presence of an oxidant and (ii) oxidant-free anaerobic oxidation of benzyl alcohols via hydride elimination. The importance lies in saving time, the exclusion of toxic metal catalysts, and reusability. Unexpectedly, in the case of C=C cleavage of styrenes, the reaction proceeds fast via an unusual Wacker-type C=C bond disruption, forming benzaldehydes with up to 92% selectivity, whereas in the case of benzyl alcohol oxidation, the mechanism involved a hydride elimination, with 100% selectivity of benzaldehyde formation. The hydride elimination reaction mechanism is supported by acetylene reduction under precise reaction conditions. Essentially, we stressed on the adaptability of using environment-friendly, effective, reusable, and single mesoporous organocatalysts in a single-pot reaction starting from the selective oxidation of benzyl alcohol to the scissoring of styrene C=C double bond into benzaldehydes.



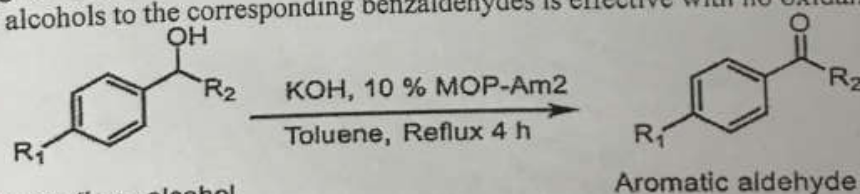
Scheme 4: Scheme 1. Synthetic Pathway of the Polymer MOP-Am2

The Brunauer–Emmett–Teller (BET) surface area analysis anticipates a type IV isotherm with a calculated surface area of 51 m²/g and a pore diameter of 1.56 nm. Oxidation of styrene usually yields 2-phenylacetaldehyde, acetophenone, and phenylepoxyde, along with minor-to-nil benzaldehyde formation. The promotion of MOP-Am2 as a metal-free catalytic bed for the oxidative C=C breakdown in the presence of TBHP as an oxidant result in the unexpected formation of benzaldehyde as the major product (Scheme 5)



Scheme 5: Regioselective C=C Bond Scission of Styrenes (for Styrene, R = H) into Benzaldehydes (in Blue Circle) Using MOP-Am2 as the Organocatalyst.

It is very interesting to note that the MOP-Am2's performance as a metal-free catalyst for the selective oxidation of benzyl alcohols to the corresponding benzaldehydes is effective with no oxidant (Scheme 6).



Scheme 6: MOP-Am2 as a Support Organocatalyst for the Oxidation of Benzyl Alcohols to the Corresponding Benzaldehydes

Thus, it indicates that MOP-Am2 having an extended conjugation of delocalized π -electrons plays an imperative role as a catalyst. Our previous study has already demonstrated how the red shift of the band gap examined by electronic absorption spectroscopy influences the performance of the π -electronic functions of 2D extended ordered polymers. It is affirmative to observe a decrease in band gaps for MOP-Am2 when compared to the basic trimer from 2.60 to 1.95 eV. This indeed enhances the probability for easy electronic transition that could promote catalysis. Thus, the effective catalytic activity of MOP-Am2 is attributed to the rich delocalization of conjugated π -electrons due to the presence of a nitrogen heteroatom, leading to a strong $\pi \cdots \pi$ or C-H $\cdots \pi$ interaction between the catalyst and styrenes or benzyl alcohols.

Date: 23rd Nov. 2021

To,
The Head, Human Resource Development Group
Council of Scientific and Industrial Research (CSIR)
CSIR Complex, Pusa
New Delhi-110012

Through: Head of the Institute

Subjects: 1. Submission of UC, SE
2. Annual progress/Closure report submission

Dear Sir,

Enclosed please find the following documents, Utilization Certificate (triplicate), Consolidated Statement of Accounts (triplicate), Progress/Closure Report, date of commencement for the research project entitled "Multicomponent Crystal Technology To Improve Drug Pharmacokinetic Attributes", sanctioned letter no. 02(0327)/17/EMR-II dated on 08/11/2017.

Thanking You,

You're faithfully

Dr. Bipul Ch. Sarma
Signature of the Principal Investigator
(Dr. Bipul Ch. Sarma), India

Signature of the Registrar, Tezpur University
(Dr. Biren Das)

Registrar
Tezpur University
Napaam, Tezpur

Declaration of Date of Commencement

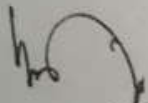
Date: 23rd Nov 2021

This is to certify that the commencement date of the CSIR project entitled, "Multicomponent Crystal Technology to Improve Drug Pharmacokinetic Attributes" with reference to sanction letter (No. 02(0327)I17/EMR-II; Dated 08-11-2017) which I received on 16-11-2017 is **01.12.2017**.

It is also declare that no other aid- giving agency is funding the work proposed to be done under the scheme sanctioned by CSIR.

Bipul Sarma
(Dr. Bipul Ch. Sarma)
Project Investigator

Dr. Bipul Sarma
Dept. of Chemical Sciences
Tezpur University
Tezpur, 781030, Assam, India


Finance Officer
Tezpur University

वित्त अधिकारी
तेजपुर विश्वविद्यालय
Finance Officer
Tezpur University

ANNEXURE-II

Consolidated Statement of Accounts
(From the date of commencement)

Title of the Research Scheme:

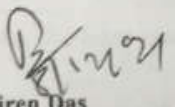
"MULTICOMPONENT CRYSTAL TECHNOLOGY TO IMPROVE DRUG PHARMACOKINETIC ATTRIBUTES"

Name of the Principal Investigator: DR. BIPUL CH. SARMA

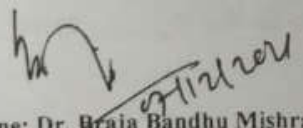
Date of Commencement: 01.12.2017

Date of Termination: 30.11.2020

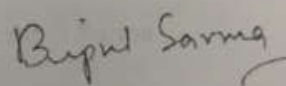
Receipts (Particulars of grants received)							Payments (Particulars of grants spent)								
Period (ending 31 st March)	Check No. Date: Amount	Contingency (Rs)	Stipend (Rs)	Scientist Allowance (for Emeritus Scientist Scheme)	Equipment Grant (Rs)	HRA+ MA	Bank Interest Accrued during (01.04.2020 to 31-03-2021)	Total (Rs)	Stipend (Rs)	Contingency (Rs)	Scientist Allowance (for Emeritus Scientist)	Equipment Grant (Rs)	HRA+ MA	Total (Rs)	Balance (Rs)
(01.04.2020 to 30-11-2020)	Letter no. 02(0327)/17/E MR-II; dated 08.11.2017 CSIR Budget head: P-81- 102 Rs.3,40,870/- Receipt on: 15.04.2021	1,90,870	1,50,000	NIL	Nil	Nil	10	3,40,880	1,50,000	2,62,097	NIL	NIL	NIL	4,12,097	-71,217


Name: Dr. Biren Das
(Registrar, Tezpur University)

Registrar
Tezpur University


Name: Dr. Braja Bandhu Mishra
(Finance Officer)

Finance Officer
Tezpur University


Name: Dr. Bipul Ch. Sarma
(P. I.)



FORM-L

UTILISATION CERTIFICATE

COUNCIL OF SCIENTIFIC AND INDUSTRIAL RESEARCH
Human Resource Development Group
CSIR Complex, Library Avenue, Pusa, New Delhi – 110012

CSIR-HRDG Scheme No. 02(0327)/17/EMR-II dated on 08/11/2017

S.No.	Particulars	Letter No. /Bank Transaction ID Nos. & Date	Amount
1	Grants received from CSIR during the year	Letter no. 02(0327)/17/EMR-II; dated 08.11.2017 CSIR Budget head: FVC/20/470/12956 BR Payment/20/470/12767 Rs.3,40,870/- Receipt on: 15.04.2021	3,40,870
2	Unspent balance of previous year (2018-2019)	-	77,733
3	Interest earned/accrued on CSIR grant (2018-2019)	-	10
TOTAL			4,18,613

1. Certified that out of Rs. 3,40,870/- (Rupees Three lakh forty thousand eight hundred seventy only) of grant-in-aid released by Extramural Research (EMR) Division of HRDG (CSIR) vide letter No./Bank Transaction ID Letter no. 02(0327)/17/EMR-II; dated 08.11.2017, CSIR Budget head: P-81-102, receipt on 15th April 2021 as given in the margin during the year and Rs. 10/- earned/accrued as interest from bank* on grants released by CSIR and Rs. 77,733/- on account of unspent balance of the previous year, a sum of Rs. 4,12,097/- has been utilized for the purpose for which it was sanctioned and that the balance of Rs. Nil remaining unutilized at the end of the year has been surrendered to EMR, HRDG (CSIR) (vide letter No. _____, DD/Cheque No. _____ dated _____)/ will be adjusted towards the grant-in-aid payable during the next year.

2. Certified that I have satisfied myself that the conditions on which the grants-in-aid was sanctioned have been duly fulfilled/are being fulfilled and that I have exercised the following checks to see that the money was actually utilized for the purpose for which it was sanctioned. The detail expenditure incurred during the year is shown in the enclosed "Statement of Accounts (Receipt & Payment)".

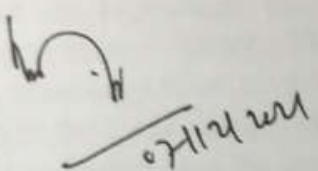
* The total interest earned during the project period for Rs 6516/- has been refunded (Demand Drafts (i) 535057, dated 17/03/2021 of Rs. 4178/- and 535362, dated 22/10/2021 of Rs. 2338.)

Page 1 of 2

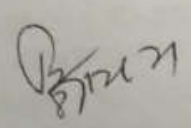
Bipul Kumar

(Kinds of checks exercised)

1. Vouchers and Statement of Accounts
2. Grant-in-Aid
3. Expenditure Register
4. Bank statements for accrual interest



Signature of Authorised Officer
with Date & Seal
Finance Officer
Tespur University



Countersigned by Registrar/Dean/Director
Of the institute with Date & Seal

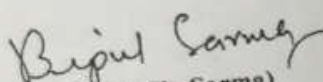
The Utilization certificate and statement should be signed by Head of the Finance & Accounts and
countersigned by Registrar/Dean/Director of the University/Institute.

Registrar
Tespur University

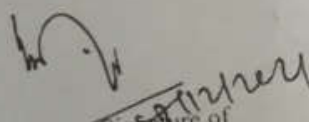
Date: 23rd Nov. 2021

UTILIZATION CERTIFICATE

Certified that the expenditure Rs. 4,12,097/- claimed under the different heads of research project entitled "*MULTICOMPONENT CRYSTAL TECHNOLOGY TO IMPROVE DRUG PHARMACOKINETIC ATTRIBUTES*", sanctioned letter no. 02(0327)/17/EMR-II dated on 08.11.2017, has actually been incurred (Staff + Contingency = Rs. 4,12,097/-) and utilized properly during the financial year 2020-2021, for which the payment was claimed and further that the grant has been exclusively utilized for the purpose for which it was sanctioned.


(Dr. Bipul Ch. Sarma)
Signature of
Principal Investigator with stamp

Dr. Bipul Ch. Sarma
Dept. of Chemical Sciences
Tezpur University
Tezpur, 784028, Assam, India


Signature of
Finance Officer, Tezpur University
with stamp
Finance Officer
Tezpur University